Detection performance assessment of the FM-based AULOS® Passive Radar for air surveillance applications

Tatiana Martelli[*], Roberta Cardinali[**], Fabiola Colone[*]

[*] DIET Dept. Sapienza University of Rome
Via Eudossiana 18, 00184 Rome, Italy
email: {tatiana.martelli, fabiola.colone }@uniroma1.it

[**]Leonardo Company
Via Tiburtina Km 12.400, 00131 Rome (Italy)
email: roberta.cardinali@ leonardocompany.com

Abstract: *In this paper, we report the latest developments obtained with the FM-based configuration of the AULOS® passive radar system designed by Leonardo SpA for air surveillance applications. Specifically, aiming at improving the target detection capability of the sensor, a robust disturbance cancellation technique is adopted. Moreover, to counteract the time-varying performance of the single FM channel, we consider the joint exploitation of multiple FM radio channels. For the purposes, the recent processing techniques developed by the research group of Sapienza University of Rome have been successfully applied. The benefits of the proposed solutions have been extensively tested and validated against both traffic of opportunity and small cooperative targets. The reported results clearly show that the choice of appropriate processing strategies is critical for the performance of the resulting system and the exploitation of effective techniques allows a significant widening of its coverage.*

1. Introduction

Nowadays, a large amount of contributions in the open literature is dedicated to investigation of passive radar (PR) systems for surveillance applications. The reason for this great interest in passive systems is that they do not emit any e.m. radiation but exploit signals from illuminators of opportunity for target detection, localization and imaging. Since they do not contribute to the e.m. pollution and they typically have a limited impact on the environment, they can be considered eco-friendly systems and are especially interesting for urban area monitoring. Moreover, the absence of an own transmitter allows reduced costs and facilitates maintenance as well as intrinsic covert operation, [1].

For all the above reasons, PR systems represent an attractive alternative to the use of the more expensive and intrusive active radars also for the industrial world. In this regard, AULOS® is the passive radar family system developed by Leonardo S.p.A.. It is a dual-band system that exploits both FM radio stations and DVB-T signals for surveillance applications. AULOS® is a technologically advanced sensor developed entirely on the basis of a "software defined radar" approach, involving signal sampling directly at carrier frequency using COTS (commercial off the shelf) devices for signal reception and digital processing. The resulting bi-band family offers great flexibility for potential use in a variety of operating conditions, along with enhanced target monitoring distance and position estimate performance, [2].

In the last years, the potential of the AULOS sensor has been mainly investigated with reference to the DVB-T based configuration. In fact, the experimental results in [3]-[5] show that the DVB-T-based PR sensor can be fruitfully employed for both coastal/maritime surveillance and air traffic control applications. Specifically, the obtained results are the fruit of a long-term collaboration between Leonardo S.p.A. and the research group at Sapienza University of Rome.

Recently, also the FM-based AULOS component received a renewed interest as it was the object of a research collaboration agreement between Nanyang Technological University (NTU) of Singapore and Leonardo S.p.A.. The aim of this collaboration project was to exploit advanced techniques for improving the performance of the FM-based passive radar.
In this paper, we show the latest results obtained with the FM-based AULOS sensor for air surveillance applications. Specifically, aiming at improving the target detection capability of the considered system, the recent processing techniques developed by the research group of Sapienza University have been implemented and tested, [6]-[7]. In fact, as it is well known, the processing scheme plays a fundamental role on the performance of a passive sensor [8]. A significant effort has been devoted to the disturbance cancellation stage which represents one of the key stages within a conventional PR processing scheme. In detail, with the term 'disturbance' we indicate the undesired contributions represented by the direct signal coming from the transmitter as well as the multipath and clutter echoes that may mask the weak targets. In addition, to counteract the time-varying performance of the single FM radio channels caused by both the broadcast radio program contents and the electromagnetic environment conditions, the joint exploitation of multiple FM channels has been considered following the approach proposed in [5], [7].
It is worth noticing that the effectiveness of the processing techniques mentioned above has been already verified by means of applications against datasets collected by experimental prototypes developed at Sapienza University. However, despite the comparative analysis with previous approaches clearly showed the benefits of the proposed solutions, the achievable performance was intrinsically limited by the simplicity of the employed hardware. Therefore, dedicated acquisition campaigns have been performed using the high performing FM-based AULOS receiver against both traffic of opportunity and small cooperative targets. By exploiting the collected datasets, we carried on an extensive analysis of the detection performance improvement provided by the proposed strategies. This allows both to quantify the advantages conveyed by the technique applied at each processing stage, and to provide a reliable assessment of the performance of the FM-based AULOS in the considered scenarios.
The paper is organized as follows. In Section 2, we report the main blocks of the FM-based AULOS processing scheme while the performed test campaigns are described in Section 3. The effect of the cancellation stage and the improvement of the detection performance provided by the multi-frequency (MF) approaches are illustrated in Section 4 and 5, respectively. Finally, our conclusions are drawn in Section 6.

2. FM-based AULOS® processing scheme

Fig. 1 sketches the optimized processing scheme for target detection of the FM-based component of the AULOS® sensor.
Two log-periodic antennas have been employed to collect the target echoes (namely, surveillance signal $s_s(t)$) while an additional antenna pointed on the transmitter is used to collect the reference signal $s_r(t)$. First, the reference signal is used to remove the undesired contributions received together with the target echoes at both available surveillance channels. To this purpose, we resort to the sliding version of the extensive cancellation algorithm (ECA-S) recently proposed by the same authors in [6].
As it is well known, the ECA basically operates by subtracting from the surveillance signal, delayed replicas of the reference signal properly weighted according to adaptively estimated coefficients [9].
Assuming that the multipath and clutter echoes are backscattered from the first K range bins and the received signals are sampled with sampling frequency *fs*, for each receiving channel the

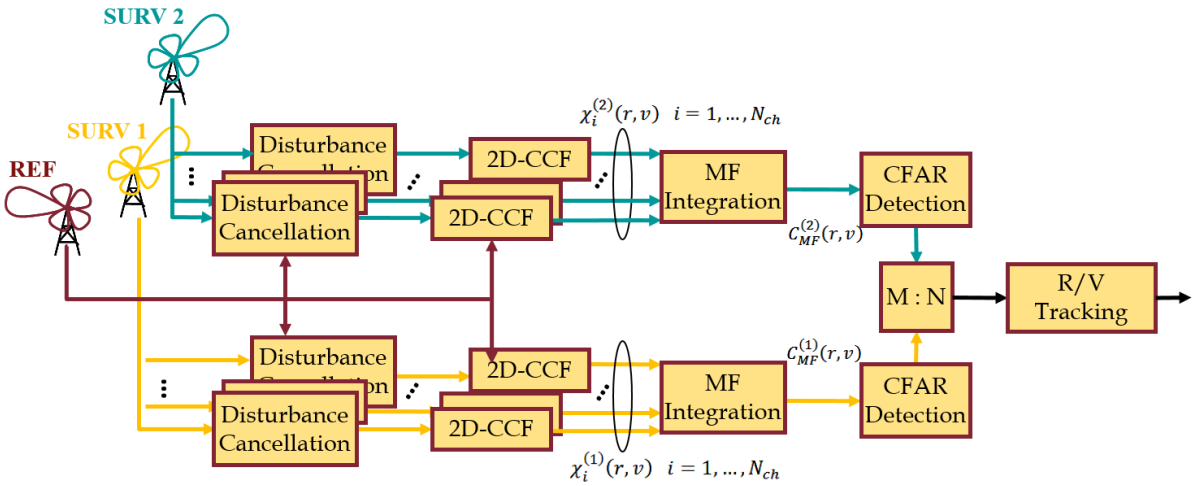

Fig. 1. FM-based AULOS® processing scheme for target detection.

output of ECA is evaluated as:

$$s_{ECA-S}[n] = s_s[n] - \sum_{k=0}^{K-1} \alpha_k s_r[n-k] \qquad n = 0, \cdots, N-1 \tag{1}$$

being N the number of samples within the coherent processing interval (CPI). The filter coefficients $\boldsymbol{\alpha} = [\alpha_0 \ \ \alpha_1 \ \cdots \ \ \alpha_{K-1}]^{\boldsymbol{T}}$ are evaluated by resorting to a Least Square (LS) approach that minimizes the power of the signal at the output of the filter:

$$\boldsymbol{\alpha} = (\mathbf{S}_r^{\mathrm{H}}\mathbf{S}_r)^{-1}\mathbf{S}_r^{\mathrm{H}}\mathbf{s}_s \tag{2}$$

where $\mathbf{s}_s$ is a $N \times 1$ vector containing N samples of the surveillance signal and $\mathbf{S}_r$ is a $N \times K$ matrix whose columns are the delayed versions of the reference signal.
In its original version, the ECA requires the filter weights to be estimated by averaging over the whole CPI. In contrast, the batch version (ECA-B) estimates and applies the filter weights over smaller portions (batches) of the integration time. Thus, ECA-B makes the system more robust to the time varying characteristics of the environment. However, as reported in [6], it yields some limitations in the presence of slowly moving targets or targets moving mainly along the cross-range direction. To overcome the above limitations, we adopt the ECA-S approach which operates over partially overlapped signal fragments [6].
Specifically, the ECA-S output at the l-th fragment of duration T_S is written as:

$$s_{ECA-S}[n] = s_s[n] - \sum_{k=0}^{K-1} \alpha_k^{(l,T_A)} s_r[n-k] \qquad \begin{matrix} n = lN_S, \ldots, (l+1)N_S - 1 \\ l = 0, \ldots, B_S - 1 \end{matrix} \tag{3}$$

where N_S is the dimension of each fragment (i.e. $N_S = T_S f_s$), $B_S = \left\lfloor \frac{N}{N_S} \right\rfloor$ is the number of consecutive fragments in the CPI, and $\boldsymbol{\alpha}^{(l,T_A)} = \left[\alpha_0^{(l,T_A)} \ \alpha_1^{(l,T_A)} \ \cdots \ \alpha_{K-1}^{(l,T_A)}\right]^T$ are the current filter coefficients. The latter are adaptively estimated on a longer signal fragment of duration $T_A = N_A/f_s$, symmetrically taken around the current signal fragment to be processed. Basically $\boldsymbol{\alpha}^{(l,T_A)}$ are evaluated as:

$$\boldsymbol{\alpha}^{(l,T_A)} = \left[\mathbf{S}_r^{(l,T_A)^H}\mathbf{S}_r^{(l,T_A)}\right]^{-1}\mathbf{S}_r^{(l,T_A)^H}\mathbf{s}_s^{(l,T_A)} \tag{4}$$

where $\mathbf{s}_s^{(l,T_A)}$ is the $(N_A \times 1)$ surveillance vector and $\mathbf{S}_r^{(l,T_A)}$ is a $N_A \times K$ matrix collecting the delayed copies of the corresponding reference signal fragment of duration T_A.

As illustrated in [6], T_A is selected to guarantee a good cancellation capability while T_S in order to move out of the Doppler range of interest (f_{Dmax}) the undesired structures that arise from the batch processing of the received signals $\left(T_S < \left(f_{Dmax} + \frac{1}{2T_A}\right)^{-1}\right)$. Obviously, with the ECA-B approach we have $T_B = T_S = T_A$.

As it is apparent, the cancellation stage has a significant impact on the detection performance of the considered passive sensor. The benefits of the ECA-S approach compared to the other versions of ECA will be illustrated in Section 4.

After the cancellation stage, the detection process is based on the evaluation of the bistatic range-velocity cross-correlation function (2D-CCF) between the output of ECA-S and the reference signal. The optimum Direct FFT technique is employed since it is the most efficient solution in the considered applications. However, to reduce the computational load, the sub-optimal Batch algorithm has been also considered by accepting limited Signal to Noise ratio (SNR) losses [10]-[11].

Despite the effectiveness of the cancellation stage, the detection performance highly depends on the time-varying characteristic of the received waveforms which largely depend on the radio program content. Since the passive sensor is able to collect simultaneously multiple FM channels, MF schemes have been implemented to enhance the target detection capability following the approaches proposed in [5], [7]. Specifically, the centralized integration scheme (SUM) is adopted. Therefore, assuming that each receiving antenna simultaneously collects N_{ch} radio frequency channels, all transmitted by the same transmitter, their 2D-CCFs are incoherently summed pixel by pixel aiming at enhancing the resulting SNR on the final integrated map $C_{MF}(r, v)$. Namely:

$$C_{MF}(r, v) = \sum_{i=1}^{N_{ch}} |\chi_i(r, v)|^2 \tag{5}$$

Once the integrated map has been evaluated at all the available surveillance channels, a conventional Cell Average Constant False Alarm Rate (CA-CFAR) threshold is separately applied to each map to detect targets with a given probability of false alarm. Notice that, the CFAR threshold should be modified taking into account the non-coherent integration over the N_{ch} frequency channels [5]. Then, an M-out-of-N criterion can be also applied to integrate the detection results obtained at the surveillance channels thus allowing a reduction in the number of false alarms. The improvement allowed by the joint exploitation of multiple frequencies with respect to the single frequency (SF) operation is analyzed in Section 5.

Finally, a target tracking algorithm is applied in the bistatic range-Doppler domain to yield more accurate measurements while reducing the false tracks.

3. Acquisition campaigns and methodology adopted for performance evaluation

To validate the effectiveness and the relative performance of the above processing scheme, dedicated acquisition campaigns have been performed against both traffic of opportunity and cooperative targets.

We report the results obtained against the datasets collected during the test campaigns in Pratica di Mare Airport, Rome. The acquisition geometry is depicted in Fig. 2. The reference antenna was steered toward the FM transmitter of Monte Cavo while two surveillance antennas (with distance $d = 1.65\ m$) were adopted with a main beam width of about 120°.

For the tests against traffic of opportunity, the surveillance antennas were pointed at 280° clockwise from north to include in the main beam the civilian air traffic departing or arriving to the Fiumicino airport. Live air traffic control registrations have been also collected (by means of an ADSB receiver, Automatic Dependent Surveillance - Broadcast). In contrast, the tests with cooperative targets were conducted pointing the surveillance antenna beam in the south direction respect the installation, specifically at 165° clockwise from north. This area was selected in cooperation with Italian Air Service Provider (ENAV), which prohibited the flight in the area near Fiumicino airport in order not to interfere with Fiumicino traffic. The tests were conducted exploiting the aircrafts provided by flying school Aviomar located in Urbe airport in Rome (see Fig. 3). Both Cessna 172 and Cessna 152 have been employed as cooperative targets equipped with a GPS receiver.

Fig. 2. Sketch of the acquisition geometry.

	Dataset #1	**Dataset #2**
Type of target	Traffic of opportunity	Cessna 172
Time duration	132 min	61 min
n° of data files	1933	729
FM channels [MHz]	103, 105.3, 105.6, 91.2, 96.1	103, 105.3, 105.6, 91.2, 92.4, 94.5

Table I. Details of the collected datasets.

During the test campaigns, different datasets have been collected. As an example, the results of two tests will be reported in the following, one for each type of targets. Each dataset is composed by consecutive data files. The total number of data files and the total time duration of each dataset together with other details about the two collected datasets are synthesized in Table I. In both cases, multiple FM radio channels have been simultaneously collected, all emitted by the same transmitter.

For the test against cooperative targets, we report the results against a Cessna 172 (see Fig. 3(a)). The GPS trajectory over the X-Y plane is also shown in Fig. 3(b). As it is evident, the maximum distance from receiver location is equal to 32 km.

To evaluate the benefits of the ECA-S approach and the MF techniques, an extended detection performance analysis has been carried out. For the test against traffic of opportunity, based on the availability of real air traffic registrations, the empirical receiver operating characteristic (ROC) curves have been evaluated to calculate the relative frequency of target detections against the measured false alarm rate parameterized by the detection threshold applied to the CFAR output map. In this paper, the analysis has been limited to targets laying in the range band [5; 100] km and two regions have been defined within this area: [5;50] km and [50 100] km. In detail, at each data file, a detection is defined as ‘correct’ when it appears at the expected range-velocity location based on the available air-truth. The detection frequency is then obtained by dividing the number of correct detections by the maximum number of target occurrences. All the remaining plots are then labeled as false alarms.

For the case of cooperative target, since a reduced amount of data is available, a quantitative analysis has been performed to evaluate the target detection performance. Specifically, we have evaluated the number of correct detections based on GPS data.

(a)

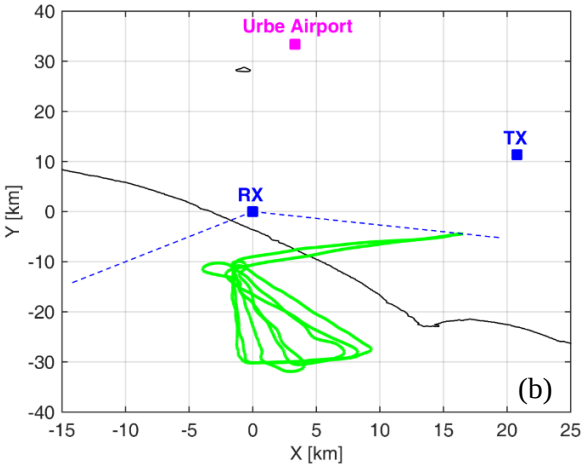

Fig. 3. Test against the cooperative target: (a) Picture of the Cessna 172; (b) GPS trajectory.

4. Impact of the cancellation stage on the detection performance

In this section, we verify the effectiveness and the improvement given by the exploitation of the ECA-S approach with respect to the previous ECA versions. For the analysis, we consider the dataset #1 against traffic of opportunity.

To this purpose, all the available data files have been first processed according to different ECA versions with K= 200 taps (i.e. 300 km at $fs = 200\ kHz$). The conventional ECA operates with T_B equal to the CPI value, namely $T_{CPI} = 1.4\ s$, while the ECA-B approach with $T_B = 0.1\ s$ which was experimentally verified to yield remarkable and quite stable cancellation performance in the considered scenario. Instead, the ECA-S technique operates with $T_S =$ 4.97 ms, to remove Doppler ambiguities appearing in the area of interest, and $T_A = 0.1\ s$ [6].

First, the disturbance cancellation capability is studied in terms of Clutter Attenuation (CA) defined as the ratio between the power levels measured, over the considered FM radio channel bandwidth, at the input and at the output of the cancellation filter. Assuming that the direct signal breakthrough and clutter are the highest contributions in the surveillance signals, the CA provides a measure of the disturbance power reduction at the surveillance channels. In the ideal case, it is limited only by thermal noise. In practice, deviations can be observed due to the presence of other undesired contributions affecting the received signal. Besides, the employed cancellation algorithm might significantly affect the performance.

As an example, Table 2 reports the CA values (obtained averaging over 50 consecutive data files) when the different algorithms are applied for the all available FM channels. As is apparent, the CA capability varies with the employed FM frequency channel. Nevertheless, in all cases, disturbance removal via ECA-B and ECA-S provides remarkably better results with respect to ECA making the system robust to slowly varying conditions of the observed scenario. Moreover, operating with ECA-S yields a slight cancellation improvement with respect to the ECA-B.

Table 2. CA values for the different FM channels when disturbance removal is performed via: conventional ECA, ECA-B and ECA-S.

	100.3 MHz	**105.3 MHz**	**105.6 MHz**	**91.2 MHz**	**96.1 MHz**
ECA	31.6 dB	24.63 dB	28.1 dB	15.86 dB	11.82 dB
ECA-B	40.6 dB	26.22 dB	31.4 dB	16.67 dB	12.55 dB
ECA-S	41.53 dB	26.25 dB	31.62 dB	16.72 dB	12.71 dB

Obviously, a higher cancellation might correspond also to a partial removal of the useful target echo. Therefore a comparison of the target detection performance allowed by different ECA versions is in order. As an example, in Fig. 4 we report the detection results of the first surveillance channel for the best FM channel at 100.3 MHz. In detail, a $T_{CPI} = 1.4\ s$ and a $P_{fa} = 10^{-4}$ have been considered. In each Figure, the red dots represent the raw detections of the PR sensor while in black is reported the available air truth for direct comparison. Notice that these are raw detections, namely no tracking or track initiation stage is applied.

As we can observe from Fig. 4(a), using the ECA for the disturbance removal, clutter residuals are observed around the zero velocity since the stationary contribution does not perfectly removed. Resorting to the ECA-B approach (see Fig. 4(b)) allows a better cancellation capability that turns out to guarantee a better continuity in target detection. As is apparent, complete plot sequences are detected and additional target tracks are correctly identified as highlighted by the green arrows. However, it is worth noticing that operating with $T_B = 0.1\ s$ yields a number of false plots at $1/T_B \cdot \lambda \cong 29\ m/s$ velocity spacing. Fig. 4(c) reports the results obtained after the disturbance removal with the ECA-S. Again, a tremendous improvement is observed with respect to the conventional ECA (targets are detected at very long bistatic range, up to 400 km) whereas comparable detection performance is obtained with respect to the ECA-B approach. However, the possibility to separately set the filter updating rate allows to avoid the many false tracks appearing in Fig. 4(b).

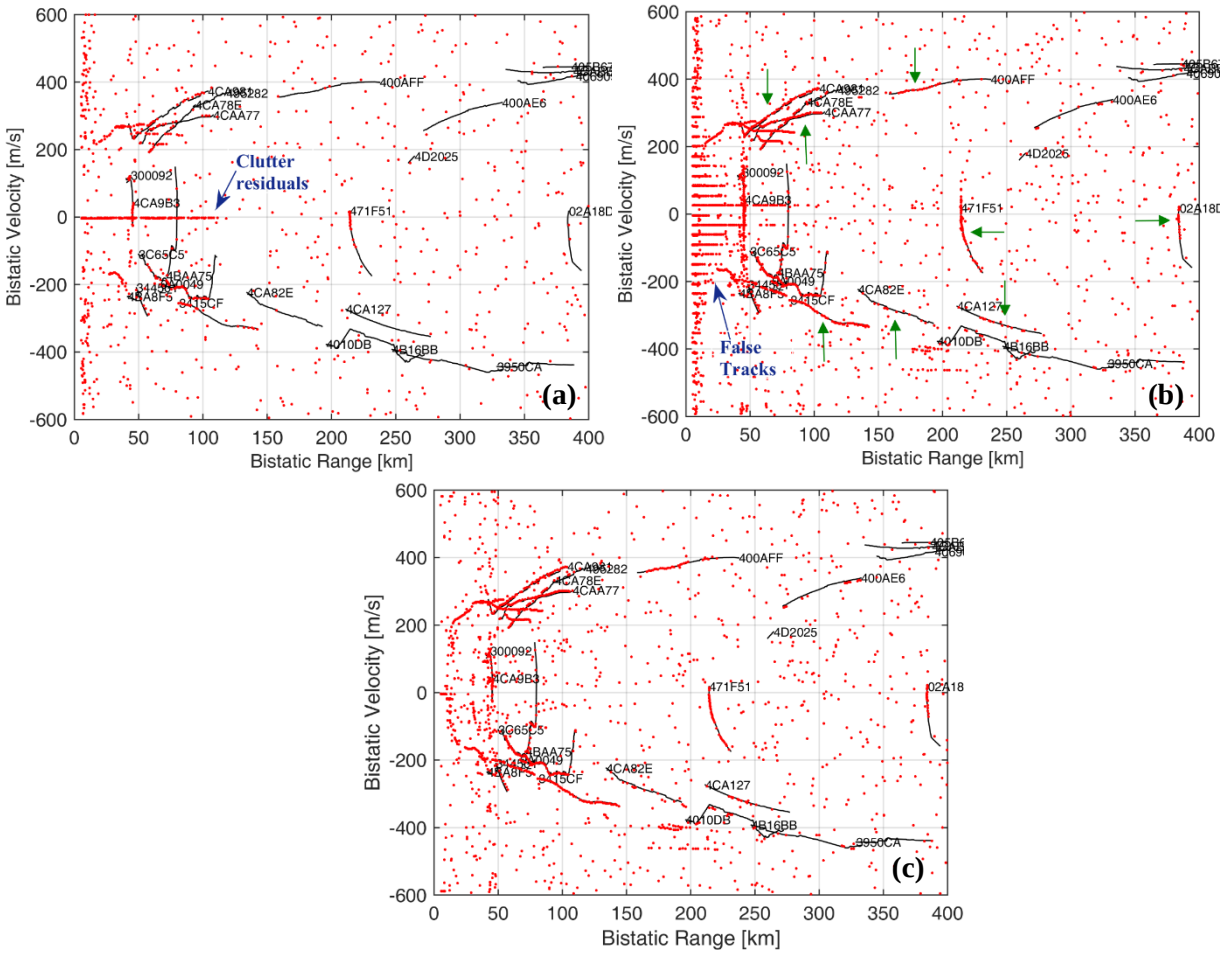

Fig. 4. Detection results over bistatic range-velocity plane against traffic of opportunity for 50 consecutive data files with the FM channel at 103 MHz when disturbance removal is performed via: (a) conventional ECA; (b) ECA-B; (c) ECA-S.

Finally, an extended detection performance analysis has been carried out by computing the ROC curves over the entire dataset composed by 1933 data files (see Table I). The results are reported in Fig. 5 for the different disturbance cancellation algorithms. We observe that the exploitation of ECA-B and ECA-S approaches allows a significant enhancement in target detection (higher than 20%) with respect to the conventional ECA. Moreover, the ECA-S yields a slight improvement compared to the ECA-B as well as it provides the additional capability to remove the false tracks.
Obviously, similar results are obtained with the other single FM channels.

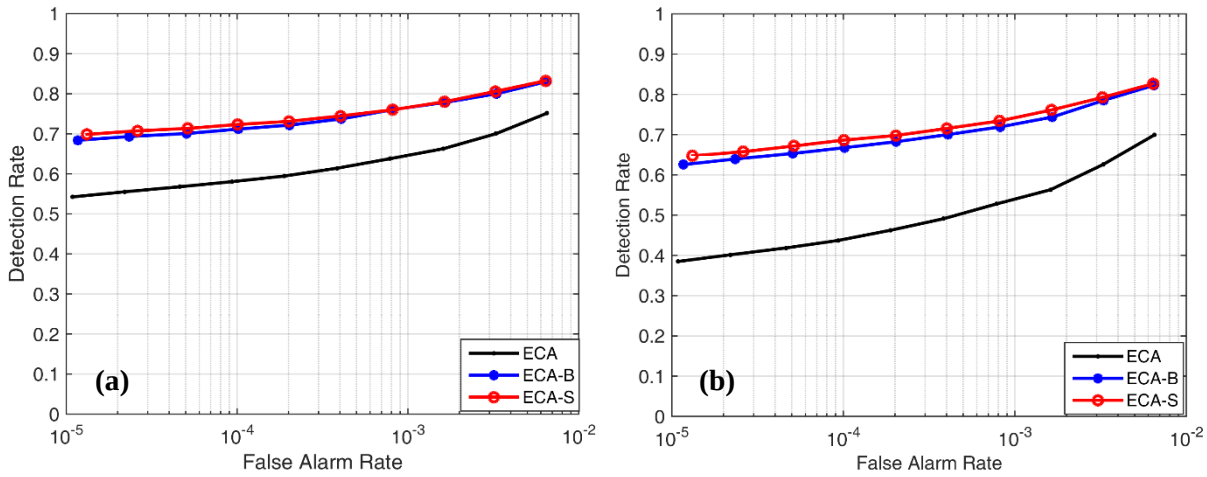

Fig. 5. ROC curves for different ECA versions in different range bands: (a) [5 50] km; (b) [50-100] km.

5. Detection performance improvement provided by the exploitation of multiple frequency channels

The benefits resulting from the application of MF approaches are here investigated against both traffic of opportunity and cooperative targets.
As it is well known, target detection capability highly varies with the employed FM channel. Obviously, a remarkable advantage with respect to the SF operation can be obtained by exploiting MF approaches [5], [7].
Against traffic of opportunity, this is illustrated in Fig. 6. For both regions, we compare the ROC curves obtained with the worst SF (96.1 MHz), the best SF (103 MHz) and the different MF configurations. Specifically, the joint exploitation of $N_{ch} = 2, 3, 4$ and 5 is considered. As for Fig. 5, the ROC curves have been evaluated on the available1933 data files. The results clearly show that the MF approaches yield a significant enhancement of the target detection capability of the PR sensor with respect to the SF operation. Among the MF approaches, the integration of all the available channels (MF-all frequencies) yields the best performance. Specifically, the improvement in the first region (see Fig. 6(a)) is limited with respect to the best SF channel (less than 10%) while a detection performance improvement of 50% is obtained with respect to the worst SF channel (namely, 50% additional target detected among the targets of opportunity). In contrast, in the region between 50 and 100 km, the improvement of the MF approach is between 20% and 50% with respect to the best SF channel. In addition, the best MF approach allows to keep the detection rate higher than 80% up to 100 bistatic km (see Fig. 6(b)).

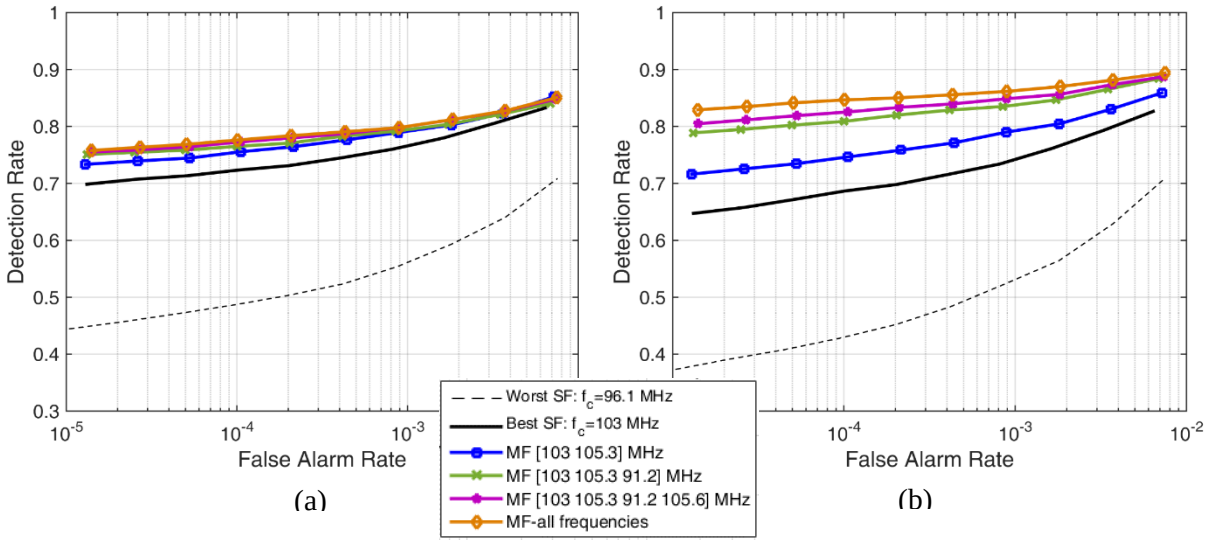

Fig. 6. ROC curves for different MF approaches compared with the best and worst SF operation for the different regions: (a) I region [5 50] km; (b) II region [50 100] km.

For the case of cooperative target, the processing scheme in Fig. 1 is applied by using a $T_{CPI} = 2$ s and a $P_{fa} = 10^{-2.5}$ at each receiving channel, thus allowing a nominal $P_{fa} = 10^{-5}$ on the final range-velocity plane after a 2-out-of-2 criterion at the two surveillance channels. The number of correct detections is reported in Table 3 when separately exploiting the six available FM channels and after the different MF integration schemes. Notice that the integration of all the available channels was not reported since the inclusion of the FM channel at 92.4 MHz does not provide a remarkable contribution. By comparing the MF detection results with those obtained with a SF operation, the detection performance improvement provided by the MF approaches is quite apparent as many additional plots are obtained. In fact, the number of correct detections moves from 313 (over 729) with the best performing SF to 461 with the best MF scheme. This is also visible in Fig. 7(a)-(b) which reports the raw detection results of the best SF and MF case, respectively. The comparison between Fig. 7(a) and Fig. 7(b) shows that the MF integration allows to detect continuously the target up to approximately 45 km, namely the coverage is extended by approximately 25% with respect to the best SF channel.

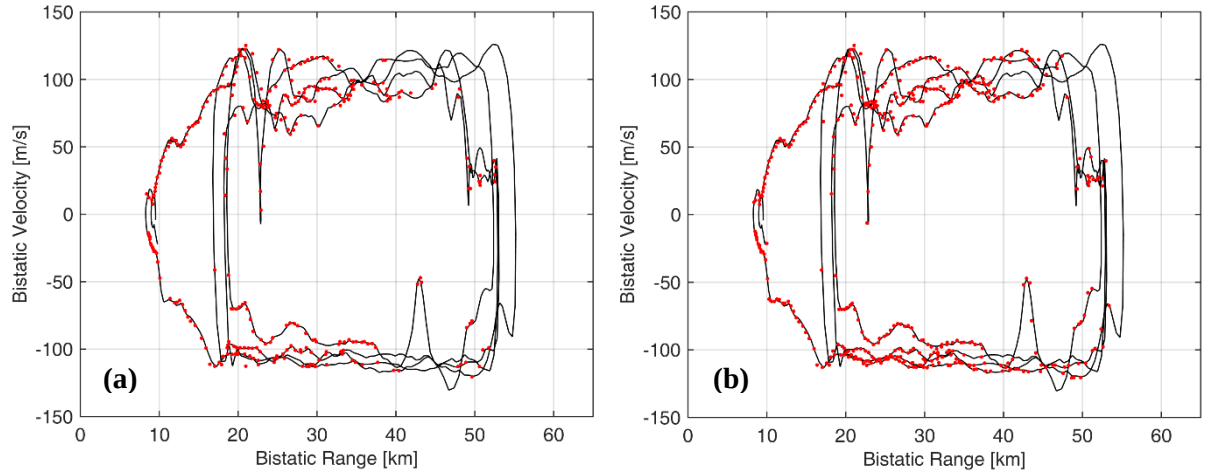

Fig. 7. Detection results over the range-velocity plane against the cooperative target: (a) best SF (105.3 MHz); (b) best MF configuration (MF [103 105.3 105.6 94.5] MHz).

Table 3. Summary of the detection results against the cooperative target.

	SF 103 MHz	SF 105.3 MHz	SF 105.6 MHz	SF 91.2 MHz	SF 92.4 MHz	SF 94.5 MHz	MF [103 105.3 105.6] MHz	MF [103 105.3 105.6 94.5] MHz	MF [103 105.3 105.6 91.2 94.5] MHz
n° detections	238	**313**	271	144	41	245	414	**461**	451

6. Conclusions

In this paper, we have reported the latest results obtained with the FM-based configuration of the AULOS® passive radar system designed by Leonardo S.p.A. for air surveillance applications. Specifically, aiming at improving the target detection capability of the considered system, the processing techniques recently developed by the research group of Sapienza University of Rome have been extensively tested and validated against both traffic of opportunity and small cooperative targets. We have conducted an extensive analysis of the detection performance improvement provided by the proposed strategies. The reported results shown that the choice of appropriate processing techniques plays a fundamental role on the performance of the high performing FM-based AULOS receiver and that the exploitation of the proposed solution allows a significant widening of its coverage.

References

[1] A. Farina and H. Kuschel, Special Issue on Passive Radar (Part I&II) – *IEEE Aerospace and Electronic Systems Magazine*, vol. 27, no. 10-11, 2012.

[2] A. Di Lallo *et al*., "AULOS: Finmeccanica family of passive sensors," in *IEEE Aerospace and Electronic Systems Magazine*, vol. 31, no. 11, pp. 24-29, November 2016.

[3] F. Colone, D. Langellotti, P. Lombardo, "DVB-T signal ambiguity function control for passive radars", *IEEE Transactions on Aerospace and Electronic Systems*, vol.50, no.1, pp. 329-347, January 2014.

[4] D. Langellotti, F. Colone, P. Lombardo, E. Tilli, M. Sedehi, and A. Farina, "Over the horizon maritime surveillance capability of DVB-T based passive radar," in *European Radar Conference (EuRAD)* 2014, Rome, Italy, October 2014.

[5] T. Martelli, F. Colone, E. Tilli. A. Di Lallo, "Multi-Frequency Target Detection Techniques for DVB-T Based Passive Radar Sensors," Sensors 2016.

[6] F. Colone, C. Palmarini, T. Martelli and E. Tilli, "Sliding extensive cancellation algorithm for disturbance removal in passive radar," in *IEEE Transactions on Aerospace and Electronic Systems*, vol. 52, no. 3, pp. 1309-1326, June 2016.

[7] F. Colone, C. Bongioanni and P. Lombardo, "Multi-frequency integration in FM radio-based passive bistatic radar. Part I: Target detection," in *IEEE Aerospace and Electronic Systems Magazine*, vol. 28, no. 4, pp. 28-39, April 2013.

[8] M. Malanowski, K. Kulpa, J. Kulpa, P. Samczynski and J. Misiurewicz, "Analysis of detection range of FM-based passive radar," *IET Radar, Sonar & Nav.*, vol. 8, no. 2, pp. 153-159, 2014.

[9] F. Colone, D. W. O'Hagan, P. Lombardo and C. J. Baker, "A Multistage Processing Algorithm for Disturbance Removal and Target Detection in Passive Bistatic Radar," in *IEEE Transactions on Aerospace and Electronic Systems*, vol. 45, no. 2, pp. 698-722, April 2009.

[10] Lombardo, P., and Colone, F., "Advanced processing methods for passive bistatic radar systems," in *Principles of Modern Radar: Advanced Radar Techniques*, W. L. Melvin, and J. A. Scheer, Raleigh, NC: SciTech Publishing, 2012.

[11] C. Moscardini, *et al*., "Batches algorithm for passive radar: a theoretical analysis," in *IEEE Transactions on Aerospace and Electronic Systems*, vol. 51, no. 2, pp. 1475-1487, April 2015.